# COMPARATIVE STUDY OF DOWNHOLE CARDS USING MODIFIED EVERITT-JENNINGS METHOD AND GIBBS METHOD

Victoria Ehimeakhe
Weatherford International

ABSTRACT
The Gibbs method has been the most widely used method for calculating downhole data in sucker rod pumping. This paper presents how the Everitt-Jennings algorithm was modified and applied to the calculation of downhole position vs. time and load vs. time data.
This modified Everitt-Jennings algorithm incorporates iteration on the net stroke and damping factor along with a fluid level calculation as part of the calculation.
This paper compares the downhole cards calculated from surface data retrieved in the lab and field, using the modified Everitt-Jennings algorithm and the Gibbs method.

## 1. INTRODUCTION AND MOTIVATIONS.

For many years, the most widely used means of artificial lift has been sucker rod pumping. Sucker rod pumping wells can be analyzed with surface dynamometer systems or more accurately with a downhole dynamometer. Unfortunately, downhole dynamometers are an expensive and impractical commodity. Therefore, it is common practice to calculate downhole data from measured surface data.

The difficulty in this approach is that the rod string is elastic and equivalent to an ideal slender bar , see [8], rendering the propagation of stress waves due to elasticity a one-dimensional phenomenon. The one-dimensional damped wave equation is most commonly used to model the behavior of the stress waves traveling down the rod string.

Other methods for solving the wave equation include the method of characteristics by Snyder, see [7], separation of variables and Fourier series by Gibbs, see [2, 3, 4], and finite difference by Knapp, see [5]. In 1976, Everitt and Jennings applied finite differences to the wave equation and outlined an algorithm for iterating on the net stroke and damping factor, see [1, 6]. The Everitt-Jennings method has been implemented and modified by Weatherford International.

The purpose of this paper is to present the modified Everitt-Jennings algorithm and offer a comparison between the modified Everitt-Jennings method and the Gibbs method. The information in this paper is presented in four parts.

In Section 2, the modifications made to the Everitt-Jennings algorithm as well as details on the implementation of the algorithm are described.

In Section 3, this paper provides a comparison between the results from the modified Everitt-Jennings algorithm and the Gibbs method and actual downhole dynamometer results using Sandia National Laboratory lab data. Sandia National Laboratory was contracted in 1990 to analyze the behavior downhole using downhole dynamometers, providing actual downhole data for six wells.

In Section 5, this paper provides a comparison between the modified Everitt-Jennings algorithm and the Gibbs method, see [2], which is widely used in the world today for calculating downhole data. The Gibbs method is currently used by Weatherford's LOWIS host analysis and optimization software and Lufkin's automation's SAM rod-pumped controller.

Conclusions follow in Section 5, while tables and figures are presented at the end of the paper.

## 2. MODIFIED EVERITT-JENNINGS.

In this section, the modified Everitt-Jennings method used to obtain the results presented in this paper is described.

## 2.1. The Everitt-Jennings method.

The key to being able to diagnose and control a rod-pumped well is the ability to simulate exactly the behavior of the rod string. However, due to the sucker rod string's elasticity, it is difficult to calculate downhole conditions from measured surface data.

The elastic force acting on the sucker rod string takes the form of stress waves traveling down the sucker rod string., As such, the sucker rod string being physically equivalent to an ideal slender bar renders the propagation of stress waves a one-dimensional phenomenon.

Downhole conditions can be correctly calculated from the surface data using the one-dimensional damped wave equation. Let $u = u(x,t)$ be the displacement of position x at time t.
The condensed one-dimensional wave equation reads:

$$v^2 \frac{\partial^2 u}{\partial x^2} = \frac{\partial^2 u}{\partial t^2} + c\frac{\partial u}{\partial t}, \tag{1}$$

where the acoustic velocity is given by: $v = \sqrt{\frac{144Eg}{\rho}}$.

It is important to note that only the damping force of the fluid nature is considered in the above equation. In theory, the damping force is a complex sum of forces acting in the direction opposing the movement of the sucker rod string, such as fluid forces and mechanical friction acting on the sucker rod string, couplings, and tubing. Friction effects are not considered here because of their dependence on unknown factors, such as deviation and corrosion damage of the rod strings. However, the fluid forces can be approximated by the viscous forces arising in the annular space.

Let $A$ be the sucker rod string's cross sectional area (in.$^2$), $\rho$ the sucker rod string's density (lbm/ft$^3$), $k$ the friction coefficient and $E$ the modulus of elasticity (psi). The gravity constant is given by $g$ (32.2 (lbm-ft)/(lbf-sec$^2$)). In order to account for varying rod diameters, (1) can be expanded as follows:

$$EA\frac{\partial^2 u}{\partial x^2}(x,t) = \frac{\rho A}{144g}\frac{\partial^2 u}{\partial t^2}(x,t) - c\frac{\rho A}{144g}\frac{\partial u}{\partial t}(x,t), \tag{2}$$

where c is the damping factor. The damping factor is described below. The wave equation is derived in detail in [6,8].

The one-dimensional wave equation was originally solved in 1967 by Gibbs, in [2], using separation of variables and truncated Fourier series. In order to solve this linear hyperbolic differential equation, Everitt and Jennings in [1] used a finite difference model.

First-order-correct forward differences and second-order-correct central differences are used as analogs for the first derivative and second derivative with respect to time respectively. A slightly rearranged second-order-correct central difference is used as the analog for the second derivative with respect to position.

The boundary conditions for the above equation are obtained directly from the surface position versus time and load versus time data. The desired solutions being only the periodic solutions, (2) does not require initial conditions, see [1]. Let $N$ be the number of recorded surface data points and $M$ be the total number of finite difference nodes along the rod string down the wellbore, such that $M$ is the last point above the pump. Let $\{i\}_1^M$ represent the vector of finite difference nodes along the rod string. Let $\{j\}_1^N$ represent the vector of sample points taken at the surface. Let $\{g_{PR}\}_1^N$ and $\{f_{PR}\}_1^N$ be the discrete functions comprised of the surface polished rod position versus time and surface polished rod load versus time data respectively.

The finite difference analogs are replaced in (2) to give:

- Initialization: For $j = 1, \cdots, N$ : $u_{0,j} = g_{PR,j}$.

- From Hooke's law: For $j = 1, \cdots, N:\ u_{1,j} = \frac{f_{PR,j} \cdot \Delta x}{EA} + u_{0,j}$.

- For $i = 2, \cdots, M$:

$$u_{i+1,j} = \frac{1}{\left(\frac{EA}{\Delta x}\right)^{+}}\left\{[\alpha(1 + c\Delta t)] \cdot u_{i,j+1} - \left[\alpha(2 + c\Delta t) - \left(\frac{EA}{\Delta x}\right)^{+} - \left(\frac{EA}{\Delta x}\right)^{-}\right] \cdot u_{i,j} + \alpha \cdot u_{i,j-1} - \left(\frac{EA}{\Delta x}\right)^{-} \cdot u_{i-1,j}\right\}, \quad (3)$$

where $\alpha = \frac{\overline{\Delta x}}{\Delta t^2}\left[\frac{\left(\frac{\rho A}{144g}\right)^{+} + \left(\frac{\rho A}{144g}\right)^{-}}{2}\right]$ and $\overline{\Delta x} = \frac{1}{2}(\Delta x^{+} + \Delta x^{-})$.

- At the pump:

$$u_{pump,j} = (1 + c\Delta t) \cdot u_{M-1,j+1} - c\Delta t \cdot u_{M-1,j} + u_{M-1,j-1} - u_{M-1,j},$$
$$F_{pump,j} = \frac{EA}{2\Delta x}\left(3u_{M,j} - 4u_{M-1,j} + u_{M-2,j}\right).$$

In the previous algorithm, $c$ is the damping factor. The stability condition associated with the above finite difference diagnostic model is as follows:

$$\frac{\Delta x}{v\Delta t} \leq 1, \quad (4)$$

where $\Delta x$ is the space between two finite difference nodes of a particular taper (ft), $\Delta t$ is the time spacing between each surface sampling point (sec.) and $v$ is the velocity of sound in the rod string (ft/sec).

Everitt and Jennings devised a method for iterating on the net stroke and damping factor in [1]. The rod string is, therefore, split into $M$ finite difference nodes of length $L_i$ (ft), density $\rho_i$ (lbm/ft$^3$) and area $A_i$ (in$^2$). The damping factor is given by:

$$c = \frac{(550)(144g)}{\sqrt{2}\pi}\frac{(H_{PR} - H_H)\tau^2}{(\sum \rho_i A_i L_i)S^2}, \quad (5)$$

Where $H_{PR}$ is the polished rod horsepower (hp), $S$ is the net stroke, $\tau$ is the period of one stroke (sec.) and $H_{hyd}$ is the hydraulic horsepower (hp) obtained as follows:

$$H_{hyd} = (7.36 \cdot 10^{-6})Q\gamma F_l, \quad (6)$$

where $Q$ is the pump production rate (B/D), $\gamma$ is the fluid specific gravity and $F_l$ is the fluid level (ft). For more details on the derivation of (5), see [1]. Everitt and Jennings proposed to first iterate on the net stroke and then iterate on the damping factor as follows:

(1) Guess at the net pump stroke (typically 90% of the surface stroke) and calculate the damping factor.
(2) Calculate the downhole data and determine the net stroke. Compare the initial net stroke with the actual net stroke.
(3) If the initial net stroke is not close enough to the actual net stroke then recalculate a new damping factor using the actual net stroke and repeat the process until convergence is achieved.
(4) Recalculate damping factor using the final net stroke.
(5) Calculate downhole data with the new damping factor.
(6) Calculate the pump horsepower $H_{pump}$ and compare it to the hydraulic horsepower $H_{hyd}$.
(7) If the pump horsepower value is not within the desired tolerance when compared to the hydraulic horsepower, update the damping factor and repeat the procedure until convergence is reached.

For details, see [1].

## 2.2. The Implementation.

In this subsection, the modifications of the initial surface data as well as modifications to the above algorithm, used for the calculations presented in this paper, are detailed.

The Everitt-Jennings algorithm gives the user the possibility of choosing the number of finite difference nodes for each taper; therefore, making it possible to output load and stress at any finite difference node down the wellbore. The code is written in such a way as to automatically compute a range of numbers of finite difference nodes satisfying the stability condition.

Also, in practice, the iteration on the net stroke and damping factor is modified. The calculation of the hydraulic horsepower requires knowing the fluid level and the pump production rate. The pump production rate is computed with:

$$Q = (0.1166)(SPM)S\,D^2,$$

where $SPM$ is the pumping unit speed (SPM), $D$ is the pump diameter ($in^2$). The net stroke, S, is unknown at the beginning of the calculation. The fluid level reflects the amount of fluid present in the wellbore annulus and may constantly change during the pumping cycle of a well. Therefore, the fluid level available may not reflect the characteristics present in the wellbore for a given stroke.

To remedy this issue, the downhole data is calculated using a fixed damping factor of 0.5. From the resulting downhole data, the net stroke is determined and the fluid level is calculated. This method provides a better first approximation of the net stroke because unlike the damping factor, the net stroke varies relatively little. Also, providing all the required input variables for the fluid level computation are correct, this method outputs a current fluid level, reflecting the conditions of the well at the time of the stroke.

Using the computed net stroke and fluid level, the hydraulic horsepower and the damping factor are computed. The iterative process for determining the net stroke and damping factor is as follows:

(1) Calculate downhole data using a fixed damping factor of 0.5.
(2) Determine the net stroke and compute the fluid level.
(3) Compute the damping factor and calculate the downhole data using the damping factor.
(4) Determine the new net stroke.
(5) If the new net stroke is within tolerance of the previous net stroke, move to the iteration on the damping factor (step 5), otherwise, go back to (step 1).
(6) Compute the damping factor using the converged net stroke value and calculate downhole data.
(7) Compute pump horsepower.
(8) If the pump horsepower value is within desired tolerance of the hydraulic horsepower, the iteration is complete. Otherwise, update the damping factor and go back to (step 2).

Providing the input variables to the fluid level calculation are accurate, the above iterative process has shown to speed up the convergence of the algorithm as well as provide more accurate downhole data. A flowchart of the process is displayed in Figure 1.

Another key aspect of the implementation is the technique used to smooth the surface data. The recorded surface data can sometimes contain too many points; therefore, introduce noise at the beginning of the computation. The first step to rectifying this problem is to truncate the data set depending on how many points compose the surface data collection.

In a second step, because the surface position versus time data is a periodic function, it can be approximated by a combination of simple sinusoidal functions. To this effect, a truncated Fourier series is used to smooth the position versus time data.

In parallel, the surface load versus time data cannot be properly approximated by a combination of simple harmonic functions; therefore it requires a different type of smoothing. The surface load versus time data is first smoothed using a least squares approach followed by a cubic spline interpolation to further smooth the data set.

It is important to note that during the implementation of the Everitt-Jennings algorithm, the data is considered to cycle on itself and therefore ghost points are created at the extremities of the data sets such that the ghost point at the origin takes the value of the last point of the data set and vice versa. This solves the problem, encountered by Everitt and Jennings in [1], of having to pick a sufficient number of data points to compensate for the data points lost from the surface to the downhole. The number of downhole output points is the same as the number of points going into the calculation.

## 3. COMPARISON WITH SANDIA NATIONAL LABORATORY DATA.

In this section, results from the modified Everitt-Jennings and Gibbs method are compared to actual downhole dynamometer data from the Sandia National Laboratory.

The Sandia National Laboratory data is a compilation of test data collected with a set of five downhole tools built by Albert Engineering under contract to Sandia National Laboratories. The necessary memory tools were deployed in the sucker rod string and equipped with sensors that were capable of measuring pressure, temperature, load and acceleration. The position was calculated by integrating the acceleration twice, yielding a load versus position downhole dynagraph. The results of these tests were presented by Waggoner in [9].

Each test conducted by the Sandia National Laboratory was designed to represent different conditions arising in the field. In Section 3.1, a well representing average conditions is analyzed. In Section 3.2, a well having fiberglass rods is considered. A Rotaflex unit is analyzed in Section 3.3 and a well with variable speed drive is analyzed in Section 3.4. Two more sets of data were analyzed by the Sandia National Laboratory, but these wells are not presented in this paper.

For each well, a description of the well is given, then a summary of Waggoner's findings and remarks, followed by the comparison to the modified Everitt-Jennings and Gibbs cards. It is important to note that the iteration on the net stroke and damping factor is not possible since the essential input variables required for that part of the code were unavailable. Each of the Figures 2 - 5b shows the surface card along with three superimposed downhole cards: the actual Sandia dynamometer reading in a dotted line, the modified Everitt-Jennings cards in a solid line, and the Gibbs card in a dashed line. Below the surface card, well information, such as pump depth, pumping unit, rod and taper information, location, and special condition for each well is given. Below the downhole card, a table containing the net stroke values, minimum and maximum loads, and average load range are given. It is important to note that the minimum and maximum loads are visually approximated as to not falsify the results by recording extreme values in the case of excess noise in the data.

### 3.1. Test Data 1: Rocky Mountain Oilfield Testing Center, Wyoming.

In this subsection, a well with as close to normal operating conditions as possible is presented.

This well has a depth of 2700' with a 0.75" API Grade 'C' steel rod string and a 1.5" RWA pump in 2.875" tubing. The pumping speed is 11 SPM with an 86" surface stroke. The dynamometer tools were installed in the rod string as follows:

1. below the pump,
2. above the pump at 2708',
3. at 2456',
4. at 1004', and
5. at 2'.

It is important to note that Tool #1 failed and no data was acquired from below the pump.
According to Waggoner [9], this well was chosen for its normal operating characteristics, representative of a fairly large number of wells. In [9], the results presented by Waggoner include dynagraph cards from the bottom of the well when the pump is full at 9:07 AM (SX1c03, 5X1c07 and 2X1c07) and when the well pumps off at 10:47 AM (SX1c05, 5X1c13 and 2X1c13). Cards were taken from data gathered at the surface, right below the polished rod and right above the pump at 2708'. Data representing a full pump and a pumped off condition at 1004' and 2056' are also available for the comparison.

The results from Tools #2, #3 and #4 were compared to results using the modified Everitt-Jennings algorithm at corresponding depths and are presented in Figure 2. The results from Tool #2 were also compared to results obtained using the Gibbs method. For Tool #4 at 1004', the shape of the Sandia downhole card and the modified Everitt-Jennings card are similar though the modified Everitt-Jennings card has an increased load span. For Tool #3 at 2456', the shapes of the cards and load ranges are similar. Above the pump, the modified Everitt-Jennings downhole card shows fewer oscillations than the Gibbs card. The shape of the modified Everitt-Jennings downhole card is similar to the Sandia card. The net stroke value of the modified Everitt-Jennings downhole card is lower by two units than the cards from the Gibbs method and Sandia data but the average load range is closer to the Sandia data than that of the Gibbs method.
For additional details about this well data and the tools used, see [9].

### 3.2. Test data 2: Mixed fiberglass/steel rod string.

In this sub-section, results from a well with combined fiberglass and steel rods are presented.

This well has a depth of 7600' with 4408' of 1.125" Norris fiberglass rods and 3200' of 1" API Grade 'D' steel rods along with a 1.5" insert pump in 2.875" tubing. The pumping speed is 8.2 SPM with a 144" surface stroke. The tools were installed in the rod string as follows:

1. below the pump,
2. above the pump at 7616',
3. 75' above the pump at 7539',
4. at the fiberglass/steel crossover at 4412', and
5. 75' above the crossover at 4335'.

According to Waggoner, this well was chosen to represent wells using fiberglass rods in general. However, the test was terminated when the rods parted after just one recording period.

Results using the modified Everitt-Jennings algorithm and the Gibbs method are compared with the results from Tool #2 at 7616' (SX2d02 and 2X2d02) in Figure 3. The net stroke values from the Gibbs and modified Everitt-Jennings methods are close together. The overall shapes of the downhole cards resemble the Sandia data even though the modified Everitt-Jennings card shows fewer oscillations than the Gibbs card.

### 3.3. Test Data 3: Rotaflex unit.

In this sub-section, a well with a Rotaflex pumping unit is considered.

This well has a depth of 9300' with an API Grade 'D' steel rod string consisting of 1" and 0.875", a 2.25" diameter tubing pump, and 2.875" tubing. The well operated at 3.9 SPM with a surface stroke of 306". During the tests, the variable frequency drive was run at 3.8, 3.5, 2.9 and 2.4 SPM. The tools were installed in the rod string as follows:

1. above the pump at 9231',
2. at 1" rods at 9089',
3. in 1" rods at 8787',
4. at the lower 0.875" rod/1" rod crossover at 7660', and
5. in the 0.875" rods at 7508'.

This well was chosen in an effort to observe the dynamics of the Rotaflex pumping unit at different pumping speeds and the dynamics of the rod string affected by the rapid direction changes during operation. In [9], results include dynagraphs cards for 3.8 SPM and 2.4 SPM. Waggoner observed that the loads and shape of the cards were similar, while the downhole stroke length was about 5% longer at the faster pumping speed. Results from above the pump using the modified Everitt-Jennings and the Gibbs method at 3.8 SPM and 2.4 SPM were compared to the Sandia results of Tool #1 at similar speeds (SX3d05, 1X3d05 and SX3d08, 1X3d08) in an effort to reproduce the longer stroke length phenomenon at the faster speed.

These results are presented in Figure 4a and 4b. In 4a, the net stroke for the Gibbs and modified Everitt-Jennings cards are similar but shorter than the Sandia net stroke. The overall card shape and average load range values are similar. Certain abnormalities at the bottom left and upper right in the Gibbs and modified Everitt-Jennings methods

are more accentuated on the Gibbs card. In 4b, the modified Everitt-Jennings card conserves the shape of the Sandia card nicely. The Gibbs card appears slanted and shows more abnormalities in the bottom left and upper right corners. The ratio of the net stroke values from 4a to 4b is conserved. (Sandia: 0.9252, modified Everitt-Jennings: 0.929 and Gibbs: 0.9288)

### 3.4. Test data 4: Varied pump speed and pump fillage test data.

In this sub-section, a well with varying pump speed and pump fillage is considered.

This well has a depth of 3100' with an API Grade 'D' steel rod string consisting of 0.875" and 0.75" rods, with 1.25" sinker bars, a 1.25" insert pump and 2.875" tubing. Tests were conducted using pump speed of 8.8, 6.7 and 4.6 SPM. The tools were installed in the rod string as follows:

1. below the pump,
2. above the pump at 3010',
3. at the sinker bar/0.75" rod crossover at 2708',
4. at the 0.75" rod/0.875" rod crossover at 1006', and
5. below the polished rod at 7508'.

According to Waggoner in [9], this well was chosen to explore the effects of both different pumping speeds and varying pump fillages on the dynamics of the sucker rod string. Results include dynagraph data from full pump fillage at 8.8 and 4.6 SPM (SX4c05, 2X4c05 and SX4c11, 1X4c11) and from pumped off conditions at the same speeds (SX3c08, 2X4c08 and SX4d05, 2X4d05).

Waggoner observed that the dynagraph data at the slower speed yields more regular downhole cards. Waggoner also remarked that the downhole tools and the surface tools were not synchronized to record data at the same time. Hence, Waggoner noticed that, in the case of the pumped off well, it was difficult to establish a uniform pumping condition over the one minute recording interval. The effect of this was that the strokes during this interval were not consistent. It was observed that even though the surface card showed about 15% pump fillage, the downhole cards at Tool #2 and Tool #1 showed pump fillages of 30% and 50% respectively.

Results using the modified Everitt-Jennings algorithm and the Gibbs method are compared to the results from Tool #2 for the full and pumped off cards at 4.6 SPM in Figures 5a and 5b. The net stroke values for the Gibbs and the modified Everitt-Jennings cards are very similar for both 5a and 5b. However in Figure 5a, the modified Everitt-Jennings downhole card shows fewer oscillations than the Gibbs downhole card, even though the average load ranges are similar. In 5b, the damping factor seems to be better adjusted in the case of the modified Everitt-Jennings card since the Gibbs card displays a vertical loop synonymous to the use of an incorrect damping factor. In both 5a and 5b, the modified Everitt-Jennings downhole card appears to be smoother than the Gibbs card. Both the modified Everitt-Jennings and the Gibbs downhole cards show 15% pump fillage in accordance with the surface card.

When applied to the Sandia data, the modified Everitt-Jennings and Gibbs show similar results though the modified Everitt-Jennings method yields smoother data with less noise. The shapes and the net stroke values of the downhole cards match up for almost every example with the exception of Test Data 3 (Figure 4b) where the Gibbs data is slanted and shows excess noise and Test Data 4 (Figure 5b) where the Gibbs data shows an ill-adjusted damping factor.

The downhole loads are dependent on the damping factor used and therefore, are a hard variable to measure. The net stroke values vary a lot less and, therefore, can be analyzed. Looking at the distributions of the absolute values of the differences between the modified Everitt-Jennings net stroke values with the Sandia net stroke values and the absolute values of the differences between the Gibbs net stroke values and the Sandia net stroke values, one can observe that the modified Everitt-Jennings net stroke values are, for the most part, closer to the Sandia data than the Gibbs data. As shown in Figure 18, which depicts the absolute values of the differences between the Sandia net stroke values and the modified Everitt-Jennings net stroke values (black) and the differences between the Sandia net stroke values and the Gibbs net stroke values (gray), the modified Everitt-Jennings net stroke values are almost consistently more accurate than those from the Gibbs method.

## 4. COMPARISON OF THE MODIFIED EVERITT-JENNINGS AND GIBBS METHOD USING FIELD DATA.

In this section, the modified Everitt-Jennings is compared to the Gibbs method using measured field data and applied to a wide variety of wells representing different conditions.

The goal of this section is to illustrate the efficiency and robustness of the modified Everitt-Jennings algorithm when applied to wells showing characteristics typical of a certain operating condition. This is an effort to demonstrate the fact that the modified Everitt-Jennings algorithm is consistent regardless of the operating conditions of a well. To this effect, a list of characteristics was compiled to represent the wide variety of well conditions arising in producing fields. Then the modified Everitt-Jennings algorithm was applied to several wells from each category and compared with the Gibbs method on those same wells. For simplicity, only one well per category is presented in this paper. The well characteristics considered are listed as follows:

1. Shallow versus deep well. In deep wells, the loads carried from the pump to the surface are increased. Therefore, the minimum and maximum loads at the surface are higher and further apart, which affects the shape of the downhole card. Most of the following examples are deep wells. Only two of the following wells are considered to be shallow with a pump depth of less than 4000'.
2. Deviated versus vertical. In deviated wells, the rod string is forced to move up and down around "corners", therefore increasing the contact between tubing and the rod string. This rod/tubing contact results in friction which causes the downhole card to appear "rounded off". This phenomenon is especially noticeable on a pumped off downhole card where the "nose" of the pumped off card will be wider or appear to be "fat".
3. High viscosity fluids. Thick, low API gravity fluids can be very thick and not flow easily. This means that the pumping system has to do extra work to move the fluid because of the added friction.
4. Different types of rod strings: steel, fiberglass, and corod. Fiberglass is used in deep wells instead of steel in order to lighten the loading on the pumping system or in wells that are highly corrosive. Corods are used in wells, which have experienced higher failure rates usually due to deviation. Corods do not have any couplings, which, therefore, reduces the friction experienced.
5. Different pumping units: conventional, Mark II, air balance and Rotaflex. Over the years, different pumping unit types have been developed, mostly to increase efficiency and to adapt to different well conditions. Mark II pumping units are advertised to be more efficient than a traditional conventional pumping unit, while an air-balanced pumping unit has a higher structure load rating than a conventional unit as well as a smaller location foot print. Rotaflex pumping units also have a smaller location foot print with available extended stroke lengths and slower pumping speeds.
6. $CO_2$ flood well.
7. Waterflood well.

For each category, several wells using actual field data are analyzed using the modified Everitt-Jennings algorithm with iteration on the net stroke and damping factor with fluid level calculation. For each of the following examples, it is possible to track the number of iterations for the net stroke and the damping factor. The iteration on the net stroke typically converges in less than five iterations while the iteration on the damping factor typically converges in nine iterations. Therefore, there exists a cutoff point such that, if the number of iterations for the damping factor exceeds eleven, then the process is stopped and the iterative process deemed unsuccessful. The iteration on the net stroke is guaranteed to succeed within the five iterations and, therefore, is not restricted. The iteration on the net stroke is said to converge when two consecutive net stroke values are less than $10^{-1}$ unit apart. The iteration on the damping factor is said to converge when the value for the hydraulic horsepower is within $10^{-1}$ of the pump horsepower value.

In each of the figures presented, the surface card is illustrated on the left, while the superimposed downhole cards for the Gibbs and modified Everitt-Jennings results are presented on the right side of the figure. The Gibbs downhole card is represented by a dotted line, while the modified Everitt-Jennings downhole card is represented by a solid line. It is important to note that the cards do not normally superimpose, but for the sake of comparison, the cards were shifted so that they superimpose.

In a table, displayed directly below each downhole card, the actual minimum and maximum loads as well as the net stroke value and average load range for each card are presented. On the left side of the figure, under the surface card, a table containing descriptive information about the well is presented. This table is displayed in an effort to

provide the reader with an overview of the well, as opposed to a full description. This information consists of well depth, pumping unit type, rod type, number of tapers, location, and which of the above listed characteristics the well belongs to. It is important to note that some wells exhibit several of these characteristics.

The Gibbs and modified Everitt-Jennings downhole cards can be compared in three ways: by their net stroke values, by their load range values, and by their shapes.

Figure 6 represents a shallow well with a depth of 3466' using a conventional pumping unit. The iteration on the net stroke converges in two iterations, while the iteration on the damping factor converges in one iteration, yielding a damping factor value of 0.065. The difference in the net stroke values is less than one unit, while the average load ranges are very close together. The shapes of the cards are also very similar.

Figure 7 represents a deviated well with a depth of 6257' using a conventional pumping unit. The iteration on the net stroke converges in three iterations, while the iteration on the damping factor converges in one iteration with a damping coefficient of 0.1. The net stroke values of the two cards are again within one unit of each other and the average load ranges values are very close together. The shapes of the downhole cards are also very similar.

Figure 8 shows a shallow well producing highly viscous fluid. The depth of this well is 796' using a conventional pumping unit. The iteration on the net stroke converges in two iterations, while the iteration on the damping factor converges in two iterations. However, the hydraulic horsepower and the pump horsepower are greater than the polished rod horsepower, which can be attributed to bad fluid data. The resulting damping factor is 0.633. The net stroke value of both cards is again within one unit of each other, while the average load range values is within one hundred units. The shapes of the downhole cards are also very similar.

Figure 9 shows a well using a corod rod string. The well has depth of 9058' and uses a Mark II pumping unit. The iteration on the net stroke converges in three iterations, while the iteration on the damping factor converges in two iterations to a damping factor value of 0.52. The net stroke value with the modified Everitt-Jennings algorithm is longer than the net stroke value obtained through the Gibbs method. The average load range with the modified Everitt-Jennings method is smaller. This can be attributed to the fact that the card produced with the Gibbs method is slanted. The modified Everitt-Jennings card, however, is horizontal and shows no slanting. In this regard, the shapes of the downhole cards are quite different.

Figure 10 represents a well using fiberglass rods. The well has a depth of 5179' and uses an air balance pumping unit. The iteration on the net stroke converges in two iterations, while the iteration on the damping factor converges in three iterations to a damping factor of value 0.511. The net stroke value obtained with the modified Everitt-Jennings is longer than the net stroke value obtained using the Gibbs method. Also, the average load ranges and the shapes of the cards are very different. The card produced with the Gibbs method is curved and concave, while the card obtained using the modified Everitt-Jennings method is more rectangular.

Figure 11 shows a well with steel rods and a depth of 6601' using a conventional pumping unit. The iteration on the net stroke converges in three iterations, while the iteration on the damping factor converges in seven iterations to a damping factor value of 0.63. The net stroke values for both cards are within two units of each other, and the average load range for the Gibbs card is greater than for the modified Everitt-Jennings method. The shapes of the downhole cards are very similar.

Figure 12 shows a well with a Mark II pumping unit with a depth of 6535'. The iteration on the net stroke converges in three iterations, while the iteration on the damping factor converges in one iteration to a damping factor value of 0.11. The net stroke value for the modified Everitt-Jennings downhole card is longer than the net stroke value for the Gibbs card, while the average load range for the modified Everitt-Jennings card is greater than the average load range for the Gibbs card. The downhole card shapes are very similar.

Figure 13 shows a well with a depth of 4610' with an air balanced pumping unit. The iteration on the net stroke converges in three iterations, while the iteration on the damping factor converges in five iterations to a damping factor value of 0.8139. The shapes of the downhole card are similar; however, the card obtained using the modified Gibbs method is “fatter”. The net stroke values for the modified Everitt-Jennings and Gibbs method are only two units apart.

Figure 14 shows a well operating with Rotaflex pumping unit at 7945'. The iteration on the net stroke converges in three iterations, while the iteration on the damping factor converges in eleven iterations such that the hydraulic horsepower is 27.58 and the pump horsepower is 27.37. The resulting damping factor value is 0.36. The shapes of the downhole cards are very similar. The net stroke obtained with the modified Everitt-Jennings method is significantly longer than the net stroke obtained with the Gibbs method and the average load range is larger.

Figure 15 shows a well using a conventional pumping unit and with a depth of 5141'. The iteration on the net stroke converges in three iterations and the iteration on the damping factor converges in seven iterations yielding in a damping factor value of 0.59. The net stroke values of each card are within one unit of each other, while the average load ranges are within one thousand units of each other. The shapes of the downhole cards are also similar although the Gibbs downhole card appears “fatter”.

Figure 16 shows a well from a $CO_2$ flood field with a depth of 5139' operating with a conventional pumping unit. The iteration on the net stroke converges in three iterations, while the iteration on the damping factor converges in one iteration, yielding a damping factor value of 0.065. The cards’ net stroke values are within two units of each other. The downhole card obtained using the modified Everitt-Jennings method is “fatter” than the Gibbs card, although the shapes are similar.

Figure 17 shows a well from a waterflood field with a depth of 4316' operating with a conventional pumping unit. The iteration on the net stroke converges in two iterations, while the iteration on the damping factor converges in 1 iteration yielding a damping factor value of 0.28. The net stroke values of each card are within one unit of each other. The average load range of the card obtained through the modified Everitt-Jennings method is larger than the load range for the Gibbs card. Even though the shapes of the downhole cards are similar, the damping factor for the Gibbs card is not adjusted properly, since the Gibbs card shows a vertical overlap.

Comparison of the net stroke values from the modified Everitt-Jennings downhole cards and the Gibbs downhole cards show that the modified Everitt-Jennings net stroke values are consistent. Figure 19 depicts the distribution of the absolute values of the net stroke differences between the Gibbs and the modified Everitt-Jennings methods for each of the examples presented above (Sandia test data and measured field data).

From Figure 19, it can be inferred that for 83% (15 of 18) of the examples, the absolute value of the differences between the modified Everitt-Jennings net stroke values and the Gibbs net stroke values is less than two units, which confirms that, for the majority of the cases, the modified Everitt-Jennings offers a similar card as the Gibbs method with a few instances where the modified Everitt-Jennings card is to be more accurate both in net stroke and damping factor estimation (loads).

When applied to measured field data, the modified Everitt-Jennings and the Gibbs method produce very similar looking downhole card shapes, though on several occasions, the modified Everitt-Jennings cards is more accurate than the Gibbs cards. For instance, in Figure 9, the Gibbs card is oddly slanted and the damping factor not adjusted properly, while the modified Everitt-Jennings card is not slanted and is more rectangular and less concave. Also in Figure 10, the Gibbs card is concave and the load range completely off, while the modified Everitt-Jennings card, though a little concave is more rectangular, horizontal and with a correct load range. In Figure 17, the damping factor for the Gibbs card is not adjusted properly because the card vertically overlaps, while the modified Everitt-Jennings card shows no overlapping.

## 5. CONCLUSIONS.

In this paper, the modified Everitt-Jennings algorithm and its implementation were described and results from the modified Everitt-Jennings method were compared to the Gibbs method using, first, actual Sandia National Laboratory downhole dynamometer readings and, second, measured field data.

When applied to the Sandia data, the modified Everitt-Jennings and Gibbs methods show similar results though the modified Everitt-Jennings method yields smoother data with less noise. The shapes and the net stroke values of the downhole cards match up for almost every example. Similar conclusions can be inferred from the results of the modified Everitt-Jennings and Gibbs methods when applied to measured field data, where the net stroke values,

shapes and load spans of the downhole cards are very similar, with the exception that the modified Everitt-Jennings algorithm offers a more accurate selection of the damping factor.

To summarize, using the modified Everitt-Jennings algorithm allows for more accurate determination of operating conditions from improved downhole pump cards, more accurate pump displacement values from calculation of the net stroke, and therefore better calculated pump efficiency values.

## BIBLIOGRAPHY.


1. Everitt, T. A. and Jennings, J. W.: "An Improved Finite-Difference Calculation of Downhole Dynamometer Cards for Sucker-Rod Pumps," paper SPE 18189 presented at the 63rd Annual Technical Conference and Exhibition, 1988.
2. Gibbs, S.G.:"Method of Determining Sucker-Rod Pump Performance," U.S. Patent No. 3,343,409 (Sept. 26, 1967).
3. Gibbs, S. G., and Neely, A. B. : "Computer Diagnosis of Down-Hole Conditions in Sucker Rod Pumping Wells," JPT (Jan. 1996) 91-98; *Trans.*, AIME,237
4. Gibbs, S. G.: "A Review of Methods for Design and Analysis of Rod Pumping Installations," SPE 9980 presented at the 1982 SPE International Petroleum Exhibition and Technical Symposium, Beijing, March 18-26.
5. Knapp, R. M.: "A Dynamic Investigation of Sucker-Rod Pumping," MS thesis, U. of Kansas, Topeka (Jan. 1969).
6. Schafer, D. J. and Jennings, J. W.: "An Investigation of Analytical and Numerical Sucker-Rod Pumping Mathematical Models," paper SPE 16919 presented at the 1987 SPE Annual Technical Conference and Exhibition, Dallas, Sept. 27-30.
7. Snyder, W. E.: "A Method for Computing Down-Hole Forces and Displacements in Oil Wells Pumped With Sucker Rods," paper 851-37-K presented at the 1963 Spring Meeting of the API Mid-Continent District Div. of Production, Amarillo, March 27-29.
8. Takács, G.: "Sucker-Rod Pumping Manual." PennWell, 2002.
9. Waggoner, J. R.: "Insights from Downhole Dynamometer Database", Southwestern Petroleum Short Course - 97.

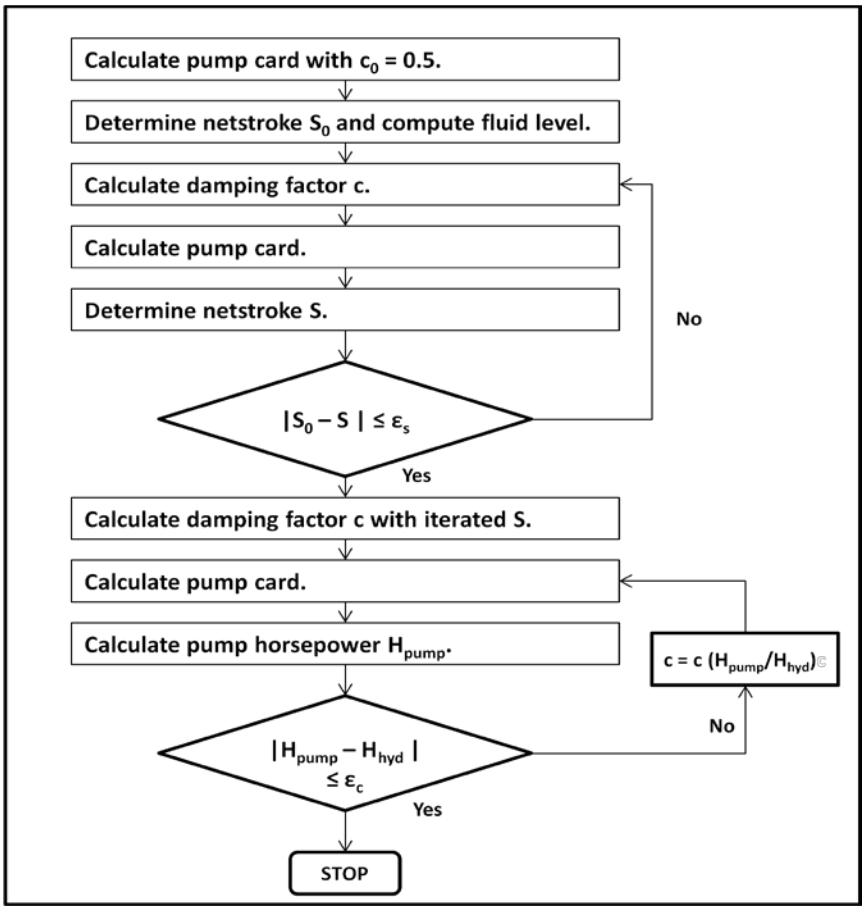


Figure 1 - Flowchart for the iteration on the net stroke and damping factor for the modified Everitt-Jennings algorithm.

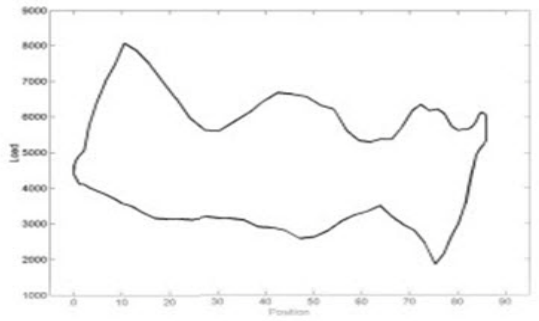


Surface Card

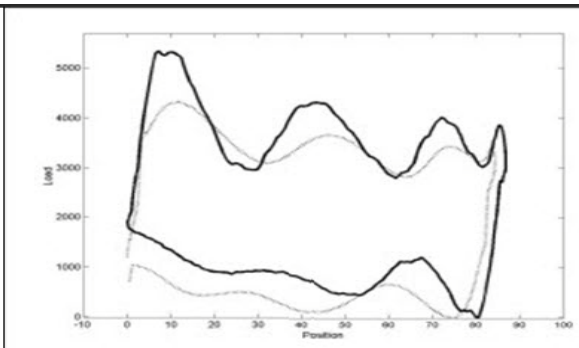


Depth 1004': Sandia (···), Everitt-Jennings (—)

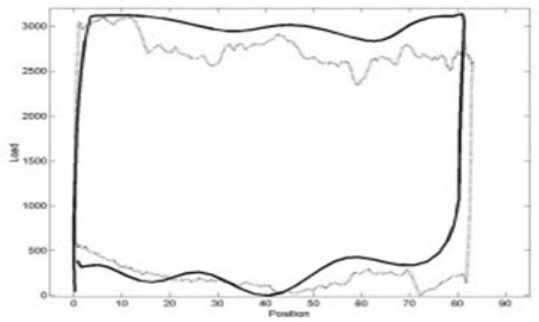


Depth 2456': Sandia (···), Everitt-Jennings (—)

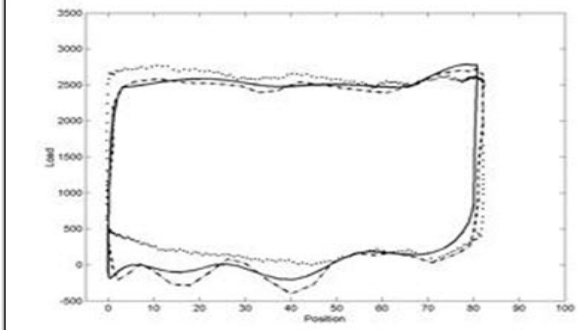


Downhole Card: Sandia (···), Everitt-Jennings (—), Gibbs (--)

Well information:
Depth: 2780'
Pumping Unit: Conventional
Rod Information: Steel 66
Taper Number: 3
Location: Wyoming
Special Condition: Normal conditions

| Test 2X1C02 | S | Min load | Max load | Avg ld range |
|---|---|---|---|---|
| Sandia | 82.08 | -637 | 1981 | 2618 |
| Everitt-Jennings | 80.7 | 334 | 2935 | 2601 |
| Gibbs | 82 | -1164 | 1589 | 2753 |

Figure 2 - Sandia Data Test 1

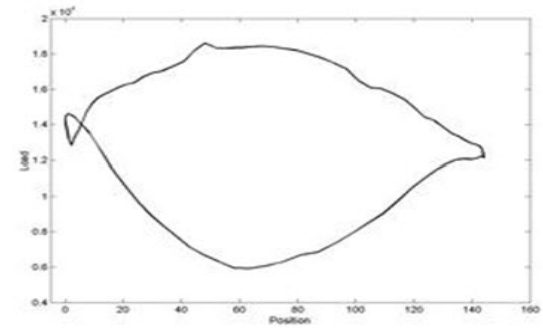


Surface Card

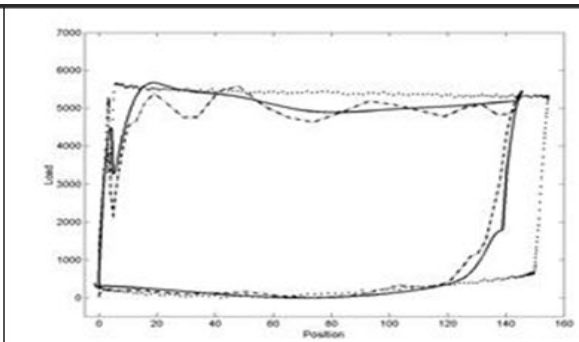


Downhole Card: Sandia (···), Everitt-Jennings (—), Gibbs (--)

Well information:
Depth: 7799'
Pumping Unit: Mark II
Rod Information: Fiberglass 10608
Taper Number: 4
Location: Unknown
Special Condition: Fiberglass rod string

| Test 2X2D02 | S | Min load | Max load | Avg ld range |
|---|---|---|---|---|
| Sandia | 154.6 | -2983 | 2422 | 5405 |
| Everitt-Jennings | 145.7 | 55 | 5867 | 5812 |
| Gibbs | 144 | -5534 | -404 | 5130 |

Figure 3 - Sandia Data Test 2

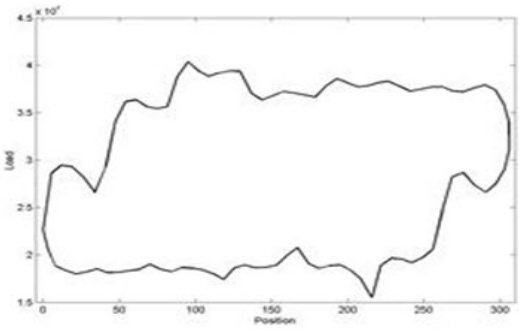


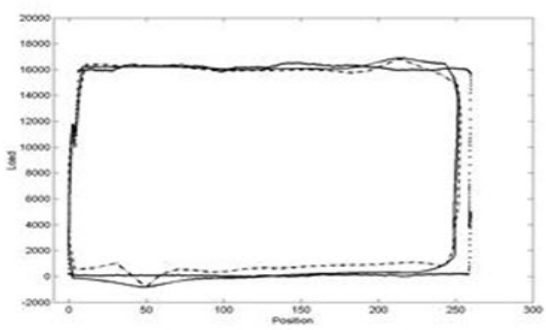


Surface Card

Downhole Card: Sandia (···), Everitt-Jennings (—), Gibbs (--)

Well information:
Depth: 9270'
Pumping Unit: Rotaflex
Rod Information: Steel 88
Taper Number: 6
Location: Unknown
Special Condition: Rotaflex pumping unit

| Test 1X3D05 | S | Min load | Max load | Avg ld range |
|---|---|---|---|---|
| Sandia | 259.72 | -2340 | 13762 | 16102 |
| Everitt-Jennings | 253.9 | 1467 | 18503 | 17036 |
| Gibbs | 253 | -4484 | 11314 | 15798 |

Figure 4a - Sandia Data Test 3 8.8 SPM

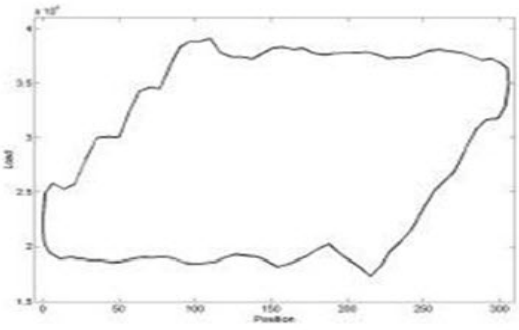


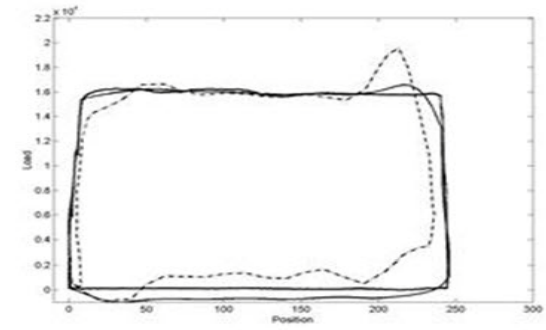


Surface Card

Downhole Card: Sandia (···), Everitt-Jennings (—), Gibbs (--)

Well information:
Depth: 9270'
Pumping Unit: Rotaflex
Rod Information: Steel 88
Taper Number: 6
Location: Unknown
Special Condition: Rotaflex pumping unit

| Test 1X3D08 | S | Min load | Max load | Avg ld range |
|---|---|---|---|---|
| Sandia | 240.31 | -2315 | 13782 | 16097 |
| Everitt-Jennings | 235.9 | 276 | 17681 | 17405 |
| Gibbs | 235 | -5623 | 14510 | 20133 |

Figure 4b - Sandia Data Test 3 4.6 SPM

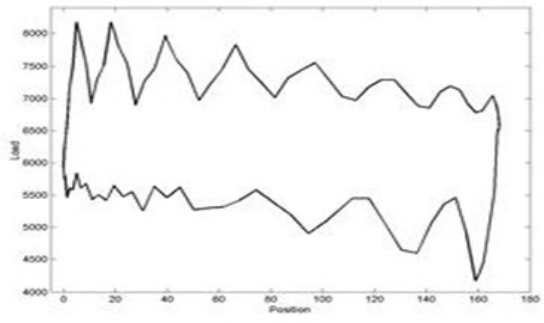


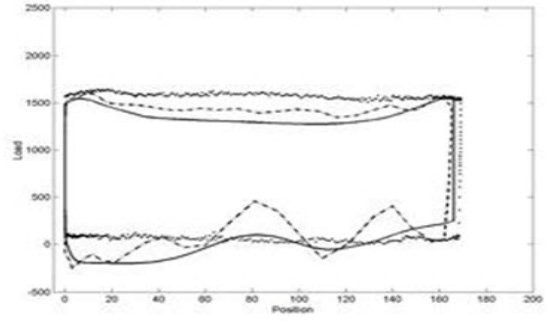


Surface Card

Downhole Card: Sandia (···), Everitt-Jennings (—), Gibbs (--)

Well information:
Depth: 3090'
Pumping Unit: Mark II
Rod Information: Steel 76
Taper Number: 3
Location: Unknown
Special Condition: Speed change

| Test 2X4C11 | S | Min load | Max load | Avg ld range |
|---|---|---|---|---|
| Sandia | 169.1 | -508 | 1049 | 1557 |
| Everitt-Jennings | 166 | 526 | 2018 | 1492 |
| Gibbs | 165 | -797 | 683 | 1480 |

Figure 5a - Sandia Data Test 4 Full Card

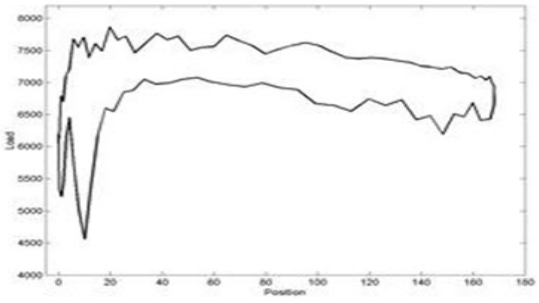


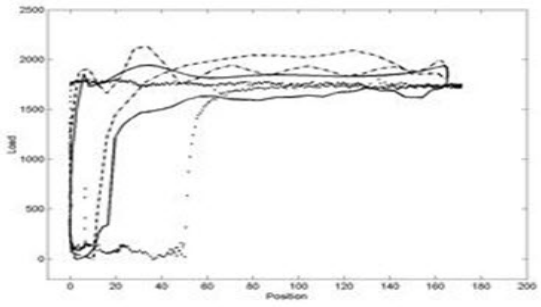


Surface Card

Downhole Card: Sandia (···), Everitt-Jennings (—), Gibbs (--)

Well information:
Depth: 3090'
Pumping Unit: Mark II
Rod Information: Steel 76
Taper Number: 6
Location: Unknown
Special Condition: Speed Change

| Test 2X4D05 | S | Min load | Max load | Avg ld range |
|---|---|---|---|---|
| Sandia | 169.24 | -502 | 1173 | 1675 |
| Everitt-Jennings | 165.2 | 132 | 2026 | 1894 |
| Gibbs | 165 | -1130 | 999 | 2129 |

Figure 5b - Sandia data Test 4 Pumped Off Card

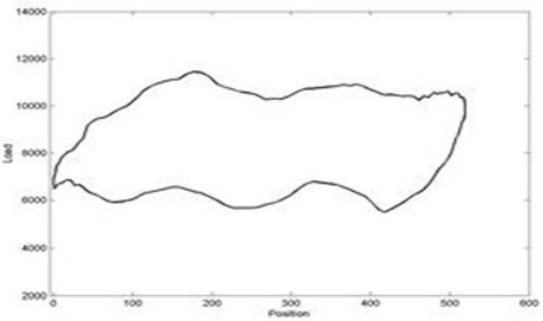


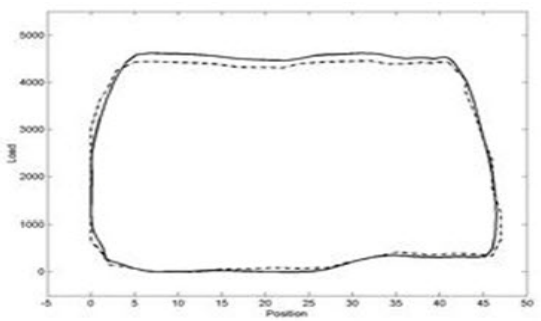


Surface Card

Downhole Card: Gibbs (···), Everitt-Jennings (—)

Well information:
Depth: 3644'
Pumping unit: Conventional
Rod information: Steel 76
Taper number: 5
Location: Unknown
Special condition: Shallow well

| | S | Min load | Max load | Avg ld range |
|---|---|---|---|---|
| Everitt-Jennings | 46.46 | -122 | 4386 | 4508 |
| Gibbs | 47 | -957 | 3263 | 4220 |

Iteration on the netstroke and damping factor
Prhp = 3.57 Damping factor = 0.065
Hydhp = 3.5 Stroke iteration = 2
Pumphp =3.49 Damping iteration = 1

Figure 6 - Shallow Well

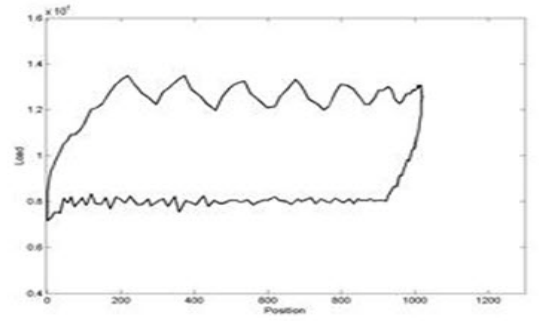


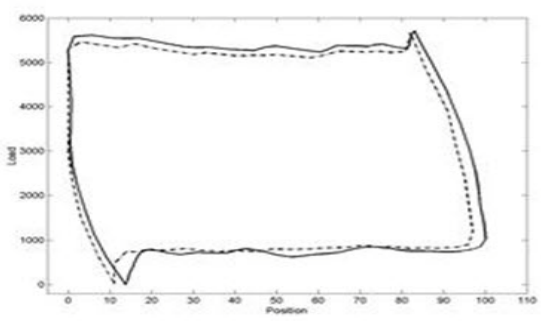


Surface Card

Downhole Card: Gibbs (···), Everitt-Jennings (—)

Well information:
Depth: 6257'
Pumping unit: Conventional
Rod information: Steel 76
Taper number: 2
Location: Mexico
Special condition: Deviated well

| | S | Min load | Max load | Avg ld range |
|---|---|---|---|---|
| Everitt-Jennings | 82.63 | -2034 | 2592 | 4626 |
| Gibbs | 82 | -3294 | 1125 | 4419 |

Iteration on the netstroke and damping factor
Prhp = 2 Damping factor = 0.1
Hydhp = 1.99 Stroke iteration = 3
Pumphp =1.92 Damping iteration = 1

Figure 7 - Well with High Deviation

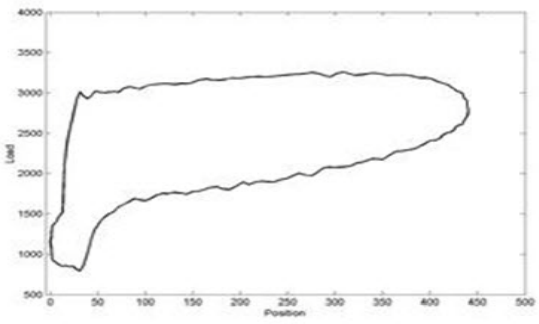


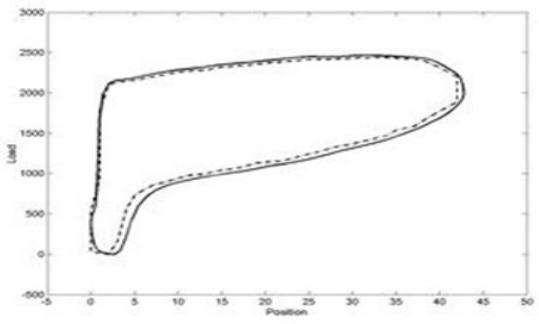


Surface Card

Downhole Card: Gibbs (···), Everitt-Jennings (—)

Well information:
Depth: 796'
Pumping unit: Conventional
Rod information: Steel 6
Taper number: 1
Location: San Joaquin Valley
Special condition: Shallow, low API gravity oil

| | S | Min load | Max load | Avg ld range |
|---|---|---|---|---|
| Everitt-Jennings | 42.73 | -333 | 2129 | 2462 |
| Gibbs | 42 | -336 | 2067 | 2433 |

Iteration on the netstroke and damping factor
Prhp = 1 Damping factor = 0.633
Hydhp = 1.48 Stroke iteration = 2
Pumphp = 1.01 Damping iteration = 2

Figure 8 - Well with Low API Gravity Oil

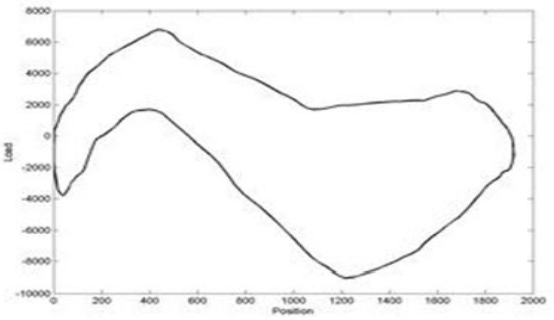


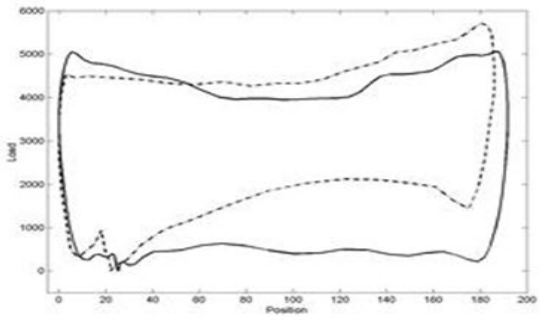


Surface Card

Downhole Card: Gibbs (···), Everitt-Jennings (—)

Well information:
Depth: 9058'
Pumping unit: Mark II
Rod information: Corod 85
Taper number: 2
Location: San Joaquin Valley
Special condition: Corod rod string

| | S | Min load | Max load | Avg ld range |
|---|---|---|---|---|
| Everitt-Jennings | 191.72 | -1108 | 3739 | 4847 |
| Gibbs | 186 | -5471 | 32 | 5503 |

Iteration on the netstroke and damping factor
Prhp = 22.65 Damping factor = 0.52
Hydhp = 10.26 Stroke iteration = 3
Pumphp =10.24 Damping iteration = 2

Figure 9 - Well with a Corod Rod String

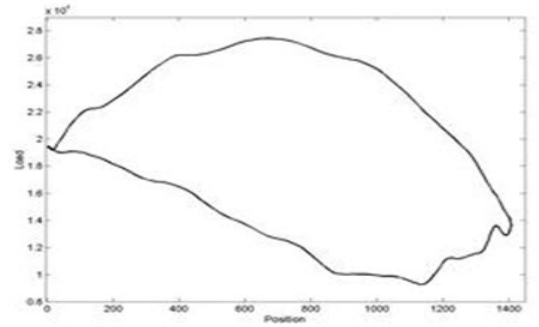


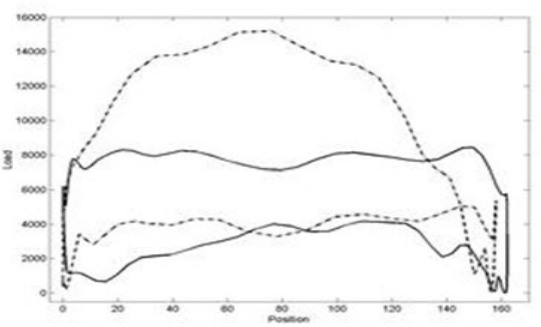


Surface Card

Downhole Card: Gibbs (···), Everitt-Jennings (—)

Well information:
Depth: 5179'
Pumping unit: Air balance
Rod information: Fiberglass 1060
Taper number: 2
Location: Permian Basin
Special condition: Fiberglass rod string

| | S | Min load | Max load | Avg ld range |
|---|---|---|---|---|
| Everitt-Jennings | 162 | -1651 | 5437 | 7088 |
| Gibbs | 158 | -1683 | 10234 | 11917 |

Iteration on the netstroke and damping factor
Prhp = 35.6 Damping factor = 0.511
Hydhp = 20.4 Stroke iteration = 2
Pumphp = 20.38 Damping iteration = 3

Figure 10 - Well with Fiberglass Rods

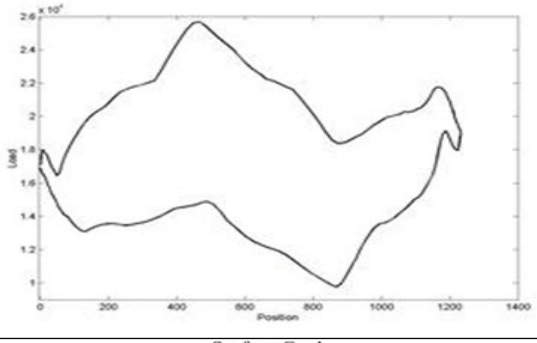


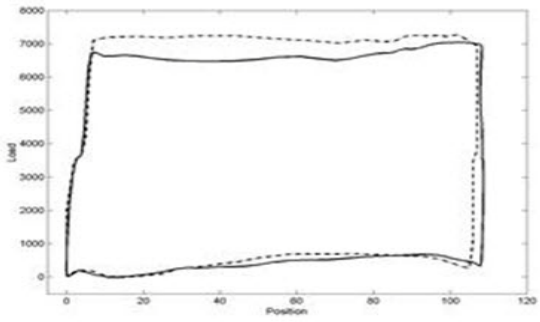


Surface Card

Downhole Card: Gibbs (···), Everitt-Jennings (—)

Well information:
Depth: 6601'
Pumping unit: Conventional
Rod information: Steel 88
Taper number: 3
Location: Permian Basin
Special condition: Steel rod string

| | S | Min load | Max load | Avg ld range |
|---|---|---|---|---|
| Everitt-Jennings | 108.64 | -877 | 5721 | 6598 |
| Gibbs | 107 | -1077 | 6069 | 7146 |

Iteration on the netstroke and damping factor
Prhp = 18.08 Damping factor = 0.63
Hydhp = 12.93 Stroke iteration = 3
Pumphp = 12.87 Damping iteration = 7

Figure 11 - Well with Steel Rods

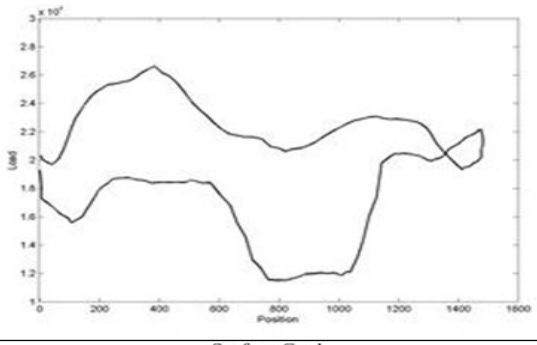


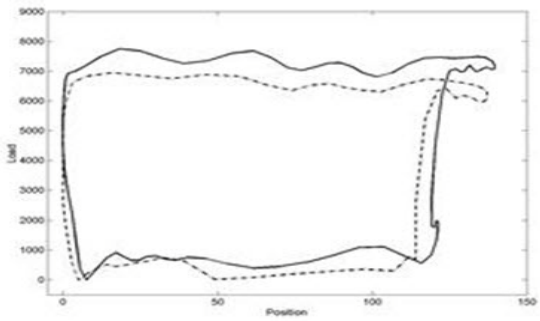


Surface Card

Downhole Card: Gibbs (···), Everitt-Jennings (—)

Well information:
Depth: 6535'
Pumping unit: Mark II
Rod information: Steel 87
Taper number: 3
Location: Permian Basin
Special condition: Mark II pumping unit

| | S | Min load | Max load | Avg ld range |
|---|---|---|---|---|
| Everitt-Jennings | 139.52 | -189 | 7090 | 7273 |
| Gibbs | 137 | -289 | 6513 | 6802 |

Iteration on the netstroke and damping factor
Prhp = 15.05 Damping factor = 0.11
Hydhp = 14.11 Stroke iteration = 3
Pumphp = 14.10 Damping iteration = 1

Figure 12 - Well with a Mark II Pumping Unit

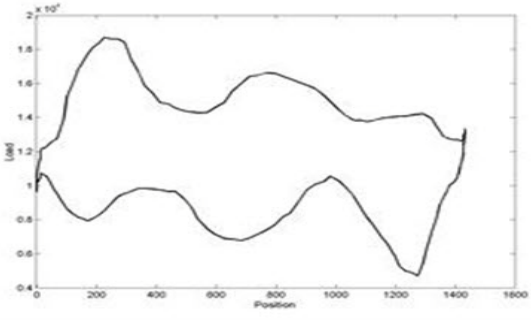


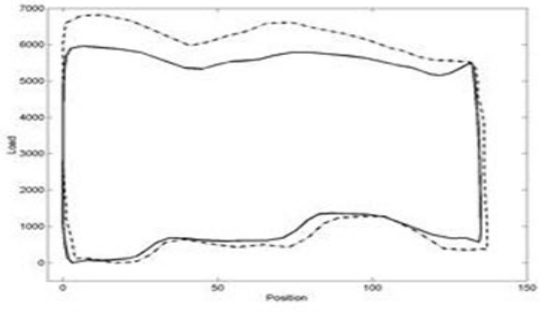


Surface Card

Downhole Card: Gibbs (···), Everitt-Jennings (—)

Well information:
Depth: 4610'
Pumping unit: Air balance
Rod information: Steel 86
Taper number: 4
Location: Permian Basin
Special condition: Air balance pumping unit

| | S | Min load | Max load | Avg ld range |
|---|---|---|---|---|
| Everitt-Jennings | 135.07 | -1047 | 4835 | 5882 |
| Gibbs | 137 | -2939 | 3851 | 6790 |

Iteration on the netstroke and damping factor
Prhp = 18.14 Damping factor = 0.8139
Hydhp = 12.49 Stroke iteration = 3
Pumphp = 12.40 Damping iteration = 5

Figure 13 - Well with an Air Balance Pumping Unit

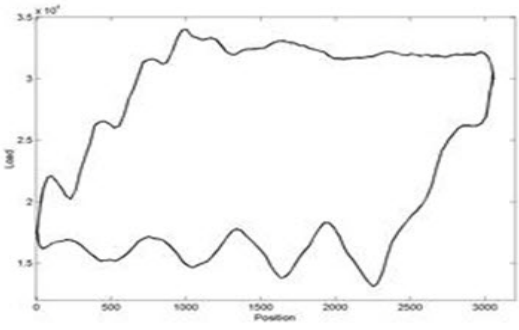


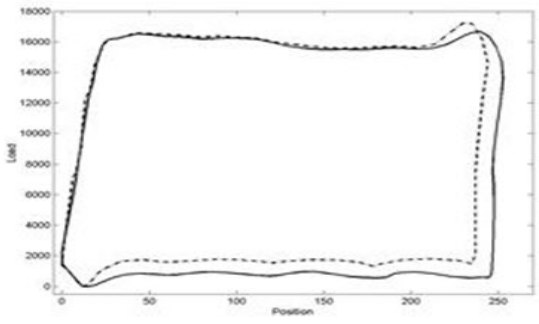


Surface Card

Downhole Card: Gibbs (···), Everitt-Jennings (—)

Well information:
Depth: 7945'
Pumping unit: Rotaflex
Rod information: Corrod 84
Taper number: 4
Location: San Joaquin Valley
Special condition: Rotaflex pumping unit

| | S | Min load | Max load | Avg ld range |
|---|---|---|---|---|
| Everitt-Jennings | 252 | -97 | 15194 | 15291 |
| Gibbs | 244 | -1136 | 13247 | 14383 |

Iteration on the netstroke and damping factor
Prhp = 29.72 Damping factor = 0.36
Hydhp = 27.58 Stroke iteration = 3
Pumphp = 27.37 Damping iteration = 11

Figure 14 - Well with Rotaflex Pumping Unit

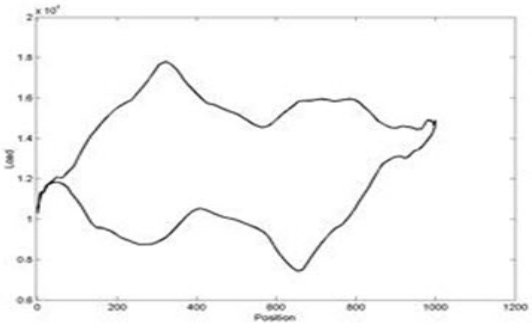


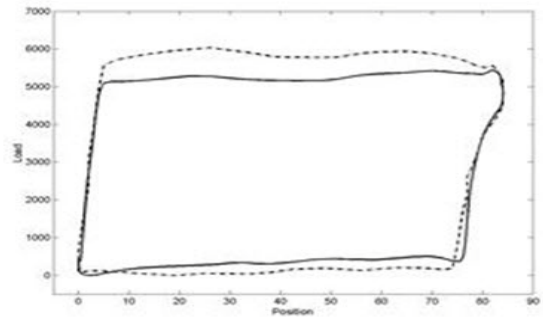


Surface Card

Downhole Card: Gibbs (···), Everitt-Jennings (—)

Well information:
Depth: 5141'
Pumping unit: Conventional
Rod information: Steel 88
Taper number: 5
Location: Permian Basin
Special condition: Conventional pumping unit

| | S | Min load | Max load | Avg ld range |
|---|---|---|---|---|
| Everitt-Jennings | 84.08 | -541 | 4540 | 5081 |
| Gibbs | 84 | -1105 | 4787 | 5892 |

Iteration on the netstroke and damping factor
Prhp = 8.74 Damping factor = 0.59
Hydhp = 6.92 Stroke iteration = 3
Pumphp = 6.82 Damping iteration = 7

Figure 15 - Well with a Conventional Pumping Unit

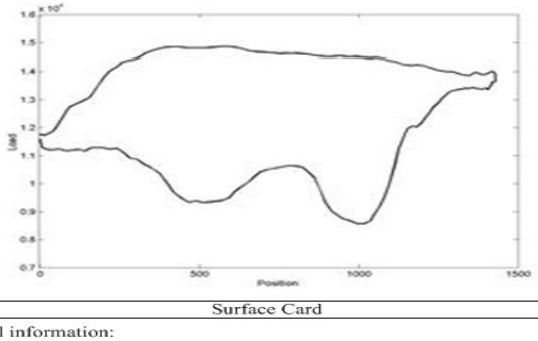


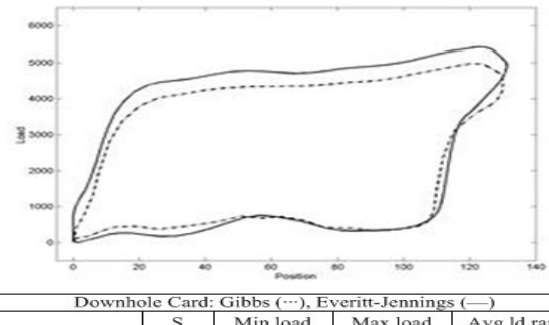


Surface Card

Downhole Card: Gibbs (···), Everitt-Jennings (—)

Well information:
Depth: 5139'
Pumping unit: Conventional
Rod information: Steel 88
Taper number: 5
Location: Permian Basin
Special condition: $CO_2$ flood well

| | S | Min load | Max load | Avg ld range |
|---|---|---|---|---|
| Everitt-Jennings | 131.17 | -890 | 4186 | 5076 |
| Gibbs | 130 | -735 | 3894 | 4629 |

Iteration on the netstroke and damping factor
Prhp = 8.22 Damping factor = 0.049
Hydhp = 8.15 Stroke iteration = 3
Pumphp =8.11 Damping iteration = 1

Figure 16 - $CO_2$ Flood Well

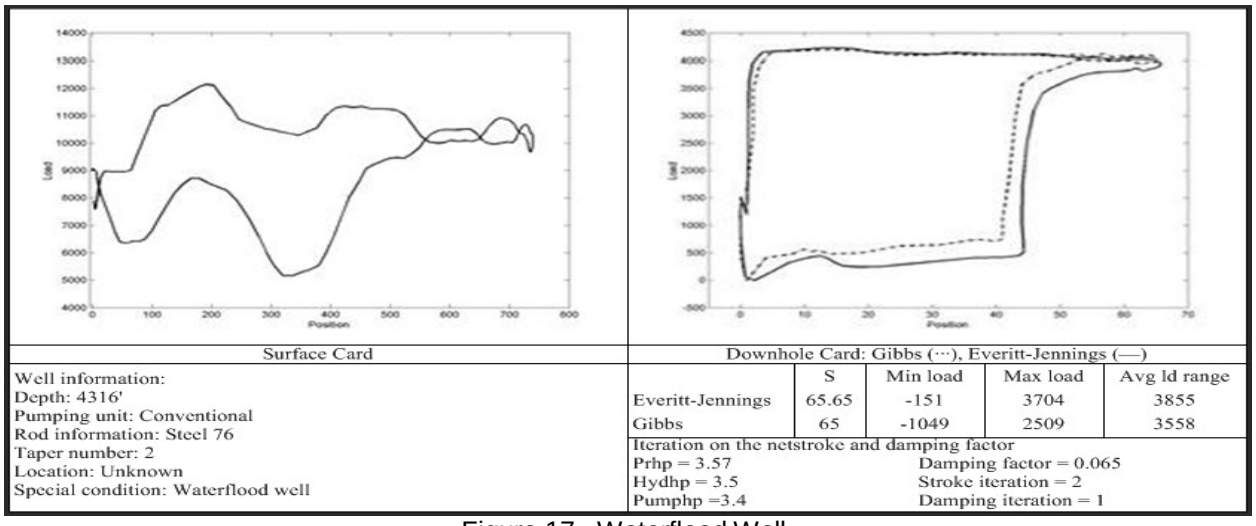


Figure 17 - Waterflood Well

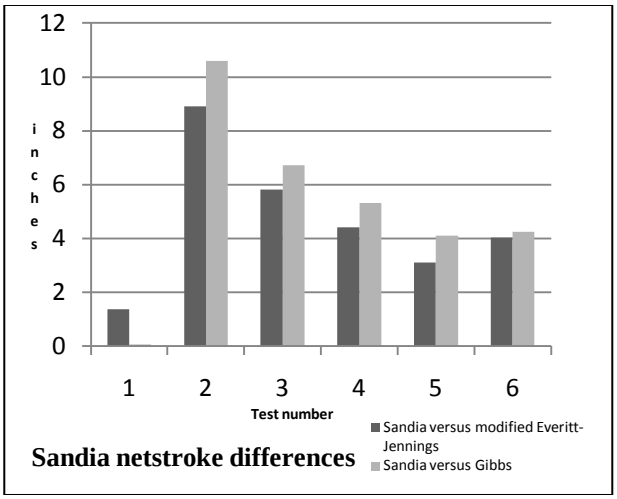


Figure 18 - Comparison of Net Stroke Values for Sandia Data

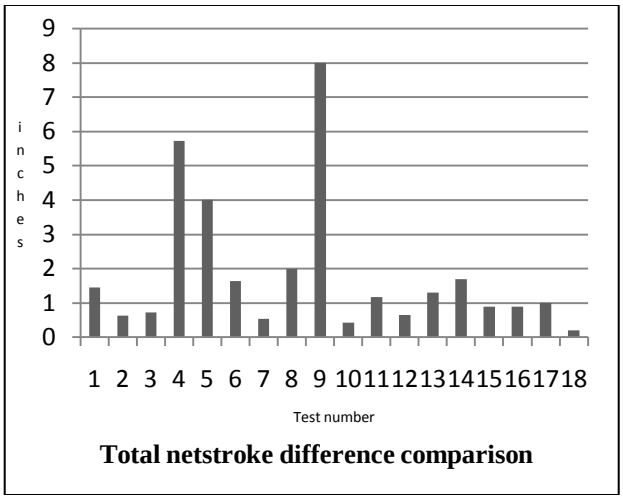


Figure 19 - Total Comparison of Net Stroke Values